DTD 5

Available online at www.sciencedirect.com
SCIENCE DIRECT®

Neuroscience Letters xxx (2005) xxx–xxx

Neuroscience Letters

www.elsevier.com/locate/neulet

Ebselen prevents noise-induced excitotoxicity and temporary threshold shift

Tatsuya Yamasoba*, Akram Pourbakht, Takashi Sakamoto, Mitsuya Suzuki

Department of Otolaryngology – Head and Neck Surgery, University of Tokyo, Hongo 7-3-1, Bunkyo-ku, Tokyo 113-8655, Japan

Received 13 October 2004; received in revised form 12 January 2005; accepted 15 January 2005

Abstract

This investigation tested the hypothesis that a noise-induced temporary threshold shift (TTS) can be attenuated by a peroxynitrite scavenger, ebselen (2-phenyl-1,2-benzisoselenazol-3(2H)-one). Guinea pigs received an oral dose of the vehicle or 10 mg/kg ebselen 1 h before exposure to 115 dB SPL 4-kHz octave band noise for 3 h. In controls, auditory brainstem response (ABR) thresholds increased by 25–45 dB immediately after noise and returned to pre-exposure baseline thresholds 7 days later. Ebselen eliminated this ABR threshold shift following noise exposure. In controls, swelling of the afferent dendrites beneath the inner hair cells was evident immediately after noise, whereas ebselen significantly reduced this pathology. These findings suggest that scavenging peroxynitrite can attenuate noise-induced excitotoxicity and, thereby, TTS.

Keywords: Guinea pig; Noise-induced hearing loss; Nitric oxide; Peroxynitrite

After exposure to intense sound, auditory thresholds can be elevated permanently, or temporarily for minutes, hours or days, depending on the parameters of acoustic overstimulation. These two phenomena, permanent (PTS) and temporary threshold shift (TTS), are dependent on mechanisms not fully understood [1,9,18]. At least two different mechanisms have been proposed for PTS: a direct mechanical trauma and a metabolic overstimulation of the cellular elements of the organ of Corti (OC). Direct mechanical trauma may damage the delicate stereocilia of the sensory hair cells or, with higher stimulation intensity, the structural integrity of the OC and basilar membrane. Intense noise exposure may also overdrive the pathways that are responsible for maintaining OC homeostasis, thus leading to metabolic changes that compromise the system. Metabolic overstimulation may be associated with biochemical traumatic processes, most notably the generation of reactive oxygen species (ROS), which may serve as triggers for necrosis or apoptosis [4,10].

Several mechanisms proposed for TTS include synaptic fatigue, metabolic fatigue of either stria vascularis or the hair cells, and changes in cochlear blood flow. Histopathological changes reported in TTS include disarrayed, splayed, fused, collapsed, or floppy stereocilia of the hair cells, buckling of the pillar bodies, and swelling of the afferent nerve terminals [9,16,17]. Postsynaptic damage in the afferent dendrites beneath the inner hair cells (IHCs) is an important component of noise-induced hearing loss [15–17], and synaptic repair mechanisms are thought to be involved in restoring function after acoustic trauma [15,17].

It has been shown that the IHCs release glutamate as a neurotransmitter activating the afferent dendrites [11] and that excess release of glutamate due to intense noise exposure causes excitotoxicity in the afferent dendrites [14]. Excess synthesis of nitric oxide (NO), which can react with $O_2^{\bullet -}$ to form highly aggressive peroxynitrite ($ONOO^-$) radicals, is known to play an important role in glutamate excitotoxicity [3,6]. Glutamate and NO can act independently or sequentially to cause excitotoxicity. NO may induce glutamate release by neurons, which then stimulates NMDA receptors and triggers excitotoxicity [8]. Conversely, when NMDA receptors are activated, Ca^{2+} influx stimulates NO production through calcium- and calmodulin-dependent neuronal nitric oxide synthase, potentially leading to neuronal death [3]. The

* Corresponding author. Tel.: +81 3 5800 8926; fax: +81 3 3814 9486.
E-mail address: tyamasoba-tky@umin.ac.jp (T. Yamasoba).

0304-3940/$ – see front matter © 2005 Elsevier Ireland Ltd. All rights reserved.
doi:10.1016/j.neulet.2005.01.047

toxic effects originally attributed to NO are now considered to be mediated mostly by the compound peroxynitrite [2]. Thus, in the present study, we tested the hypothesis that ebselen, a glutathione peroxidase mimic and a scavenger of peroxynitrite, attenuates noise-induced excitotoxicity and TTS.

Twenty-four male albino guinea pigs (250–350 g), with normal auditory brainstem response (ABR) thresholds at 2, 4, 8 and 16 kHz, were randomly divided into vehicle-treated ($n = 14$) and ebselen-treated experimental groups ($n = 10$). These animals received an oral dose of 0.25 ml of 99% chloroform solution alone (vehicle) or containing 10 mg/kg ebselen one hour before exposure to noise. Ten mg/kg of ebselen was selected because this dose most effectively attenuates PTS in guinea pigs [13]. The animals were subjected to a 3-h noise exposure (115 dB SPL, 4-kHz octave band noise) generated within a single-walled, sound-deadened chamber. Two separately caged animals were tested at one time and allowed to move freely during exposure. The sound chamber was fitted with speakers driven by a noise generator and power amplifier. A 0.5-in. Bruel and Kjaer condenser microphone and a fast Fourier transform analyzer were used to measure and calibrate the sound level at various locations within the chamber to ensure stimulus uniformity within ±1 dB.

Five animals in each group underwent ABR measurements immediately and 1, 3, 7, and 14 days after noise exposure to assess the effect of ebselen on TTS. The method of ABR measurement has been described previously [13]. In brief, animals were anesthetized with a mixture of xylazine hydrochloride (10 mg/kg, i.m.) and ketamine hydrochloride (40 mg/kg, i.m.), and needle electrodes were placed subcutaneously at the vertex (active electrode), beneath the pinna of the measured ear (reference electrode), and beneath the opposite ear (ground). The stimulus duration was 15 ms; the presentation rate, 11/s; and the rise/fall time, 1 ms. Responses of 1024 sweeps were averaged at each intensity level (5 dB steps) to assess threshold. Threshold was defined as the lowest intensity level at which a clear reproducible waveform was visible in the trace.

Four animals given vehicle alone were euthanized under deep anesthesia with xylazine hydrochloride and ketamine hydrochloride 7 days after noise exposure to assess hair cell damage. Two animals unexposed to noise served as controls. The cochleae were perfused intrascalarly with 4% paraformaldehyde and immersed in the same fixative overnight. The surface of the organ of Corti was stained with rhodamine phalloidin and each turn of the cochlea was observed under fluorescent microscope as previously described [13]. The influence of ebselen on noise-induced morphological changes in the cochlea was examined in the remaining animals ($n = 5$ in each group). These animals were deeply anesthetized with a mixture of xylazine hydrochloride and ketamine hydrochloride immediately after the termination of noise exposure. The left bulla was then exposed and the perilymphatic spaces perfused for 10 min with 2% paraformaldehyde in 2.5% glutaraldehyde. The animals were then sacrificed and the left cochlea quickly removed, immersed in the same fixative for 24 h, and decalcified in 10% ethylenediaminetetraacetic acid for 14 days. The specimens were post-fixed in 1% osmium tetroxide for 2 h, dehydrated in a graded series of ethanol, and embedded in epoxy resin. Ultra-thin sections were obtained from the very upper part of the basal turn corresponding to the region most responsive to frequencies in the range of 4–6 kHz and observed under transmission electron microscope (TEM). We focused on the histological changes in the stria vascularis, the hair cells and supporting cells, and the afferent dendrites beneath the IHCs. Because the extent of swelling of the afferent dendrites was obviously different between vehicle- and ebselen-treated animals, we compared the area (μm^2) of the swollen dendrites in the two groups. In each animal, a total of 10 sections that contained the nucleus of different IHC were collected. From these, five sections were chosen randomly for measuring and statistical analysis by a blinded technician who did not know the aim of the current study. The images of these sections were captured using a scanner, the area of the swollen dendrites measured using Adobe Photoshop image analysis software, and the mean of the areas calculated. Student's t-test was used for statistical analysis.

The experimental protocol was approved by the University Committee for the Use and Care of Animals at the University of Tokyo and conforms to the National Institute of Health Guide for the Care and Use of Laboratory Animals.

ABR thresholds before noise exposure were essentially equivalent among all animals. In vehicle-treated controls, ABR thresholds were moderately increased immediately after noise; the threshold shifts were approximately 25 dB at 2 kHz and 45 dB at 4, 8, and 16 kHz. The ABR thresholds then showed gradual recovery, returning to pre-exposure baseline thresholds 7 days later, indicating that the noise exposure induced a TTS. In contrast, ebselen-treated animals showed virtually no ABR threshold shifts after noise (Fig. 1). The ABR thresholds shifts immediately after noise were significantly different ($p < 0.001$) at all frequencies measured between control and ebselen-treated animals. The IHCs and outer hair cells (OHCs) were well preserved in both vehicle-treated noise-exposed animals and unexposed controls; the number of missing OHCs in the lower two turns was 6.4 ± 2.5 in the former and 4.9 ± 4.4 in the latter, suggestive that the noise used did not cause hair cell death.

In controls that were euthanized immediately after noise, the OC in the upper basal turn showed numerous swollen dendrites beneath the IHCs. In contrast, pathological changes were quite limited in ebselen-treated animals (Fig. 2). The mean area of swollen dendrites was significantly smaller ($p < 0.01$) in ebselen-treated animals compared to controls. In neither controls or ebselen-treated animals sacrificed immediately after noise exposure was there obvious evidence of other pathological changes reported to be correlated to TTS, such as edema or vasoconstriction in the stria vascularis, buckling of the pillar bodies, or fusion or loss of stereocilia.

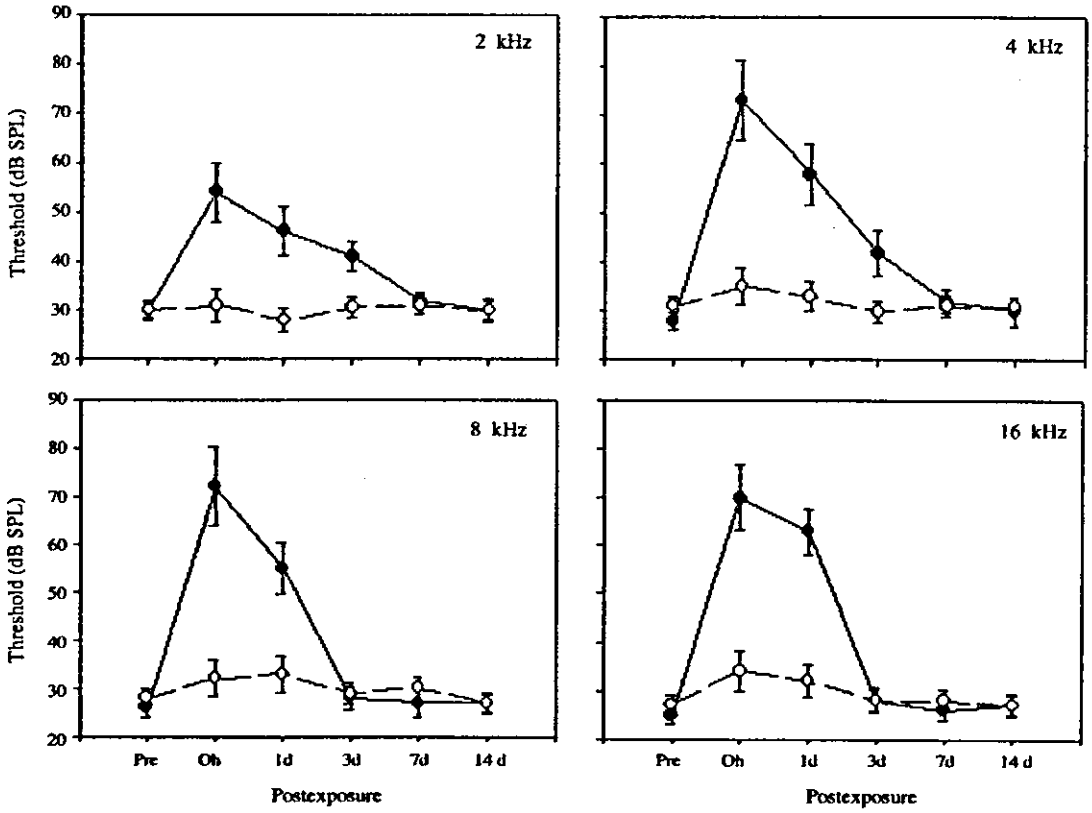

Fig. 1. Thresholds of auditory brainstem response (mean ± S.D.) measured before and immediately and 1, 3, 7, and 14 days following noise exposure in vehicle-treated controls (●) and ebselen-treated animals (○).

The current study shows that ebselen virtually prevents noise-induced TTS under conditions where vehicle-treated controls developed a TTS of approximately 25–45 dB. TEM observation revealed that immediately after noise, the afferent dendrites beneath the IHCs were severely swollen in control animals, whereas such pathological changes were significantly reduced in ebselen-treated animals. Other pathological changes were not evident in either controls or ebselen-treated animals. Because we did not examine otoacoustic emissions or use scanning electron microscopy, it is possible that functional and/or subtle anatomical changes in the regions other than the afferent dendrite, especially the OHCs, were missed. However, the above findings indicate that ebselen can attenuate noise-induced changes at least in the afferent dendrites beneath the IHCs and thereby TTS.

Using fluorescent dye 4,5-diaminofluorescein diacetate, it has been shown that in the normal guinea pig cochlea, NO is present in the afferent nerves and their putative endings near the IHCs, putative efferent nerve endings near the OHCs, the IHCs and OHCs, and blood vessels [20], and that inducible NO synthase (iNOS) is expressed in cochlear nerve fibers, as well as in hair cell stereocilia, Hensen's cells, and the stria vascularis [19]. It has also been reported that, when exposed to broadband noise (3 h/day at 110 or 120 dB SPL) for three consecutive days, NO concentration is increased in the perilymph, NO fluorescence becomes more intense in the IHCs and OHCs [21], and iNOS fluorescence signals becomes more intense in cochlear tissues compared to unexposed controls [19]. In addition, it has been reported that cochlear perfusion with kainic acid (KA), a conformationally restricted analog of glutamate known to have excitotoxic effects on spiral ganglion cells, causes significant elevation of thresholds of the cochlear nerve compound action potential and that this threshold shift is significantly reduced by pretreatment with nitroindazole, a competitive inhibitor of neuronal NOS [6]. The toxic effects originally attributed to NO are now regarded to be mediated mostly by the compound peroxynitrite [2]. Considering these findings, it is likely that ebselen attenuated noise-induced excitotoxicity and thereby TTS, by scavenging peroxynitrite formed by the reaction between noise-induced $O_2^{\bullet -}$ and NO.

It may also be possible that ebselen attenuated TTS because of its antioxidant property. It has been shown, however, that topical application of R-PIA, which increases endogenous antioxidant levels, to the chinchilla cochlea facilitates the recovery of hearing function 4 days after noise exposure but does not attenuate initial noise-induced threshold shifts [5]. Ohinata et al. [10] have shown that lipid peroxidation (8-isoprostane formation) in the OC induced by intense noise is significantly attenuated by *N*-methyl-D-aspartate (NMDA) receptor antagonists and anti-oxidant *N*-acetylcysteine, but not by NOS inhibitor, L-*N* (omega)-nitroarginine methyl

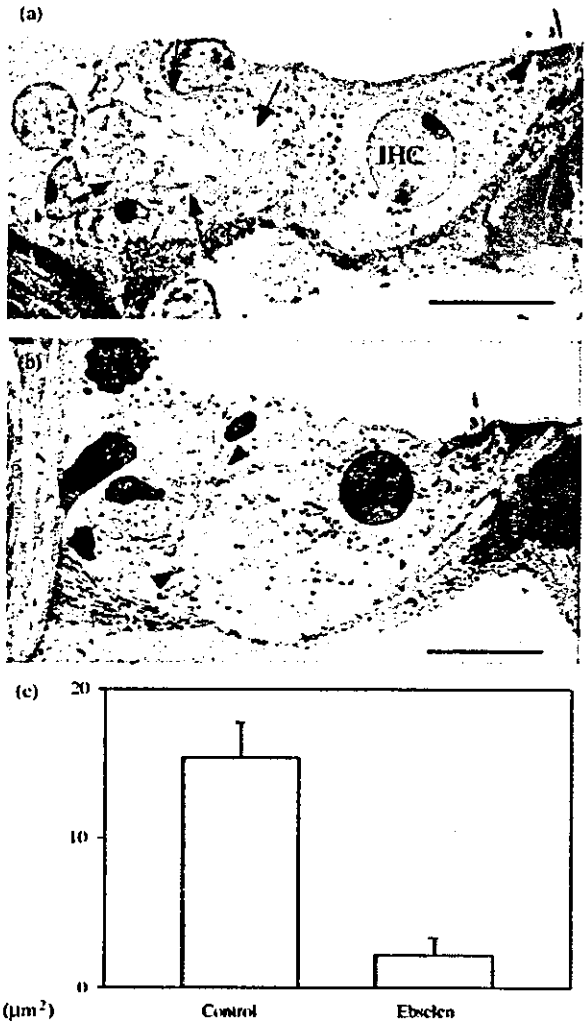

Fig. 2. Typical transmission electron microscopic findings in the medial side of the organ of Corti immediately following noise exposure in vehicle-treated controls (a) and ebselen-treated animals (b). The afferent dendrites are markedly swollen in vehicle-treated controls (arrows) but relatively normal in ebselen-treated animals (arrowheads). The bar indicates 10 μm; IHC: inner hair cell. (c) The mean ± S.D. of areas (μm²) of the swollen afferent dendrites in the vehicle-treated control and ebselen-treated animals.

ester. Therefore, it is unlikely that ebselen's protective effect against TTS is provided chiefly by scavenging ROS or reducing ROS formation in the OC.

In conclusion, the current study shows that ebselen can prevent noise-induced excitotoxicity and thereby TTS. This prevention likely reflects ebselen's scavenging of peroxynitrite, thus supporting the view that peroxynitrite, at least in part, mediates excitotoxicity induced by intense noise. It has previously been shown that ebselen can also attenuate PTS in guinea pigs [13] and rats [7]. Since ebselen has already been used in humans clinically to treat ischemic stroke with few or no side effects [12], our findings reinforce the potential clinical utility of ebselen to prevent and/or treat noise-induced hearing loss in humans.

Acknowledgements

We thank Prof. J.M. Miller, Kresge Hearing Research Institute, University of Michigan, for helpful comments and discussion and Mr. Y. Mori for technical support. This work was supported by a grant (15110201) from the Ministry of Health, Labour and Welfare, Japan to T.Y., and a grant (13470357) from the Ministry of Education, Culture, Sports, Science and Technology, Japan to T.Y.

References

[1] W.W. Clark, Recent studies of temporary threshold shift (TTS) and permanent threshold shift (PTS) in animals, J. Acoust. Soc. Am. 90 (1991) 155–163.
[2] J.P. Crow, J.S. Beckman, The role of peroxynitrite in nitric oxide mediated toxicity, Curr. Top. Microbiol. Immunol. 196 (1995) 53–73.
[3] V.L. Dawson, T.M. Dawson, E.D. London, D.S. Bredt, S.H. Snyder, Nitric oxide mediates glutamate neurotoxicity in primary cortical cultures, Proc. Natl. Acad. Sci. U.S.A. 88 (1991) 6368–6371.
[4] D. Henderson, S.L. McFadden, C.C. Liu, N. Hight, X.Y. Zheng, The role of antioxidants in protection from impulse noise, Ann. N. Y. Acad. Sci. 884 (1999) 368–380.
[5] B.H. Hu, X.Y. Zheng, S.L. McFadden, R.D. Kopke, D. Henderson, *R*-Phenylisopropyladenosine attenuates noise-induced hearing loss in the chinchilla, Hear. Res. 113 (1997) 198–206.
[6] K.L. Johnson, V. Carrasco, J. Prazma, C.J. Zdanski, W.F. Durland, H.C. Pillsbury, Role of nitric oxide in kainic acid-induced elevation of cochlear compound action potential thresholds, Acta Otolaryngol. (Stockh.) 118 (1998) 660–665.
[7] E.D. Lynch, R. Gu, C. Pierce, J. Kil, Ebselen-mediated protection from single and repeated noise exposure in rat, Laryngoscope 114 (2004) 333–337.
[8] P.R. Montague, C.D. Gancayco, M.J. Winn, R.B. Marchase, M.J. Friedlander, Role of NO production in NMDA receptor-mediated neurotransmitter release in cerebral cortex, Science 263 (1994) 973–977.
[9] A.S. Nordman, B.A. Bohne, G.W. Harding, Histopathological differences between temporary and permanent threshold shift, Hear. Res. 139 (2000) 13–30.
[10] Y. Ohinata, J.M. Miller, J. Schacht, Protection from noise-induced lipid peroxidation and hair cell loss in the cochlea, Brain Res. 966 (2003) 265–273.
[11] O.P. Ottersen, Y. Takumi, A. Matsubara, A.S. Landsend, J.H. Laake, S. Usami, Molecular organization of a type of peripheral glutamate synapse: the afferent synapses of hair cells in the inner ear, Prog. Neurobiol. 54 (1998) 127–148.
[12] M.J. Parnham, H. Sies, Ebselen: prospective therapy for cerebral ischemia, Exp. Opin. Investig. Drugs 9 (2000) 607–619.
[13] A. Pourbakht, T. Yamasoba, Ebselen attenuates cochlear damage caused by acoustic trauma, Hear. Res. 181 (2003) 100–108.
[14] J.L. Puel, C. Gervais d'Aldin, S. Saffiedine, M. Eybalin, R. Pujol, Excitotoxicity and plasticity of IHC—auditory nerve contributes to both temporary and permanent threshold shift, in: A. Axelsson, H.M. Borchgrevink, R.P. Hamernik, P.A. Hellström, D. Henderson, R.L. Salvi (Eds.), Scientific Basis of Noise-induced Hearing Loss, Thieme, New York, 1996, pp. 36–42.
[15] J.L. Puel, S. Saffiedine, C. Gervais d'Aldin, M. Eybalin, R. Pujol, Synaptic regeneration and functional recovery after excitotoxic injury in the guinea pig cochlea, C. R. Acad. Sci. III 318 (1995) 67–75.
[16] R. Pujol, J.L. Puel, Excitotoxicity, synaptic repair, and functional recovery in the mammalian cochlea: a review of recent findings, Ann. N. Y. Acad. Sci. 884 (1999) 249–254.

[17] D. Robertson, Functional significance of dendrite swelling after loud sounds in the guinea pig cochlea, Hear. Res. 9 (1983) 263–278.

[18] J.C. Saunders, E.C. Yale, Y.M. Szmyko, The structural and functional consequences of acoustic injury in the cochlea and peripheral auditory system: a five year update, J. Acoust. Soc. Am. 90 (1991) 136–146.

[19] X. Shi, C. Dai, A.L. Nuttall, Altered expression of inducible nitric oxide synthase (iNOS) in the cochlea, Hear. Res. 177 (2003) 43–52.

[20] X. Shi, T. Ren, A.L. Nuttall, Nitric oxide distribution and production in the guinea pig cochlea, Hear. Res. 153 (2001) 23–31.

[21] X. Shi, T. Ren, A.L. Nuttall, The electrochemical and fluorescence detection of nitric oxide in the cochlea and its increase following loud sound, Hear. Res. 164 (2002) 49–58.

The Journal of Laryngology & Otology
July 2004, Vol. **120**, pp. 546–550

Clinical Records

Ototoxicity after use of neomycin eardrops is unrelated to A1555G point mutation in mitochondrial DNA

TATSUYA YAMASOBA, M.D., KATSUNORI TSUKUDA*, M.D.

Abstract
Ear drops containing neomycin only rarely cause ototoxicity. The authors report on three patients with a tympanic membrane perforation who developed severe ototoxicity after use of eardrops containing 0.35 per cent neomycin. Mitochondrial DNA analysis revealed that there was no A1555G point mutation in these patients. This finding indicates that application of low concentration neomycin to the middle ear can cause severe inner ear damage even in humans who are not hyper-susceptible to aminoglycosides.

Key words: Neomycin; Cochlea; Hearing Loss, Sensorineural; Vertigo; Mutation; Drug Hypersensitivity

Introduction

Neomycin is one of the most ototoxic drugs in modern medicine. Neomycin ototoxicity has been reported in all the routes of administration: oral, rectal, parenteral, intrapleural, wound irrigation, and aerosol spray. Neomycin primarily causes cochlear damage, especially when renal and gastrointestinal functions are altered.[1] Hearing impairment may develop, or continue to progress after systemic or topical application is discontinued.[1,2] Kavanagh and McCabe[1] reviewed cases of neomycin ototoxicity and concluded as follows: 'the usual latency is from two to six weeks after the onset of neomycin therapy. Since many patients received short courses of the drug, the hearing loss was often noticed days to weeks after the drug was discontinued. The onset of deafness may be severe and sudden but is usually progressive and may progress from six to 10 months, leaving the patient with a profound hearing loss.'

Several commonly used eardrops, including Cortisporin®, contain neomycin. When applied to the middle-ear space of guinea pigs, neomycin readily entered the perilymph in the cochlea through the round membrane[3] and at a concentration of 5 mg/ml or more caused dose-dependent ototoxicity.[4,5] Despite these experimental findings, hearing loss, vertigo, or both have rarely been reported after use of a neomycin otic suspension. Several large reference works failed to find such cases in humans (reviewed by Lind and Kristiansen[6]). An inquiry made by Swiss otolaryngologists showed that inner ear damage caused by antibiotic eardrops with ototoxic properties is estimated to occur in only one of 1 000 to 3 000 treatments.[7] Merifield *et al.*[8] found no increase in the bone conduction thresholds in 44 children with chronic suppurative otitis media treated with five different topical aminoglycosides, four of which contained neomycin at a concentration of 0.33 or 0.35 per cent. Lind and Kristiansen,[6] however, reported that a patient with a ventilation tube to the middle ear developed severe hearing loss and vertigo after the use of eardrops containing 5 mg/ml neomycin. These findings suggest that humans may be less susceptible to neomycin applied topically to middle-ear spaces than are guinea pigs. Neomycin at the concentration of 0.35 per cent or less applied to middle-ear spaces may not be sufficient to cause inner ear damage in humans.

In Japan, Rindelon A® ear drops (Shionogi Co. Ltd.), which contain 0.35 per cent neomycin sulphate and 0.1 per cent betamethasone sodium phosphate in a 5 ml aqueous solution, are very commonly used. Approximately 19 000 000 bottles of these eardrops are sold annually in Japan. Despite the low concentration of neomycin, otologists know that this preparation may cause, albeit very rarely, inner ear damage. Why eardrops with low concentration neomycin are ototoxic in a limited number of cases is not known. The easy access of a neomycin otic suspension to the round window membrane in the absence of inflammatory oedema and secretion in the middle ear is considered a significant factor in producing this side effect.[6] Another possibility is that patients who experience inner ear damage after the use of a neomycin otic suspension may have hyper-susceptibility to aminoglycosides. Persons with an A-to-G transition at nucleotide (nt) 1555 of the 12S ribosomal RNA gene in the mitochondrial DNA (mtDNA) are reported to be very

From the Department of Otolaryngology Head and Neck Surgery, University of Tokyo, and the Third Department of Internal Medicine*, University of Tokyo, Tokyo, Japan.
Accepted for publication: 7 March 2004

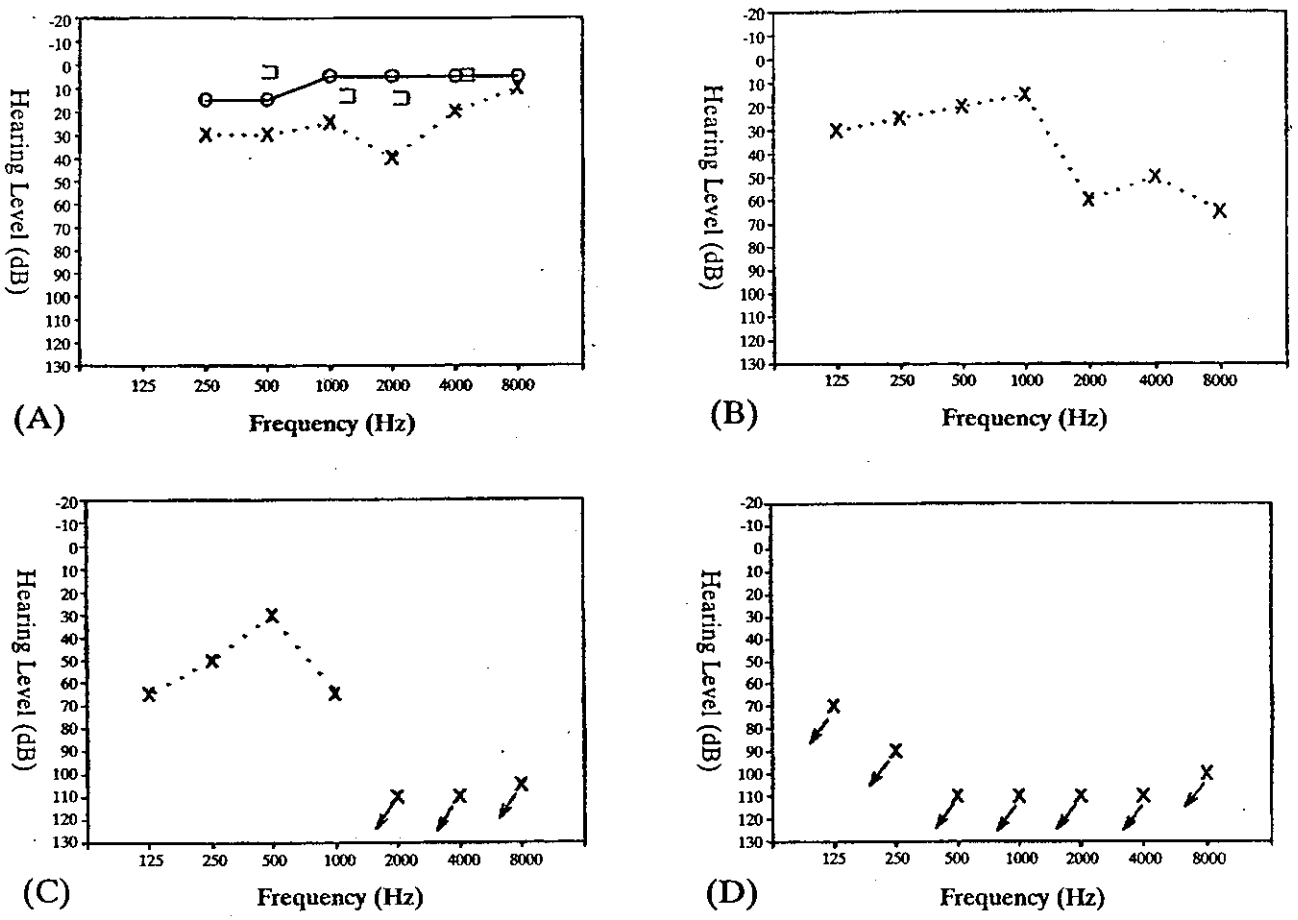

FIG. 1

Pure-tone audiograms for *Case 1*. (a) Slight conductive hearing loss on the left before use of Rindelon A® eardrops. (b) Sensorineural hearing loss at higher frequencies after the use of four bottles of the ear drops. (c) Progression of sensorineural hearing loss at all frequencies three months after cessation of eardrops use. (d) Complete deafness nine months after the use of Rindelon ® eardrops.

susceptible to aminoglycosides.[9-12] The authors therefore investigated whether ototoxicity caused by a neomycin otic suspension was closely related to the presence of the A1555G mutation.

Case reports

Case 1

A 50-year-old female suffering from tinnitus and mild hearing loss in the left ear, which had appeared one month before, visited the authors' clinic. She had been given six bottles of Rindelon A® ear drops over a three-month period at a private ENT clinic because of a slight serous discharge from her left ear. A pure-tone audiometric examination made before application of Rindelon A® ear drops showed mild conductive hearing loss on the left (Figure 1(a)). An otoscopic examination found a small perforation in the inferior part of the left tympanic membrane through which the mucoperiostium on the promontory looked intact. No discharge was present in the middle or external ear. A pure-tone audiometric examination showed an increase in hearing thresholds on the left at high frequencies (Figure 1(b)). Neuro-otological examinations found no abnormalities. An electronystagmogram (ENG) recorded no spontaneous, positional, or positioning systems. A caloric testing with 5 ml cold (4°C) saline produced nystagmus with a slow component velocity of approximately 35°/s in both ears. Magnetic resonance imaging (MRI) with Gd-DTPA enhancement excluded intracranial lesions such as a cerebellopontine angle (CPA) tumour. Although use of these eardrops was stopped, over the next six months her left-side hearing gradually worsened (Figures 1(c), 1(d)). Oral administrations of coenzyme Q, ATP and/or vitamin B12 were not effective. Nine months later, she was completely deaf in the involved ear.

Case 2

A 54-year-old male had been treated for one year for otitis media with effusion in the left ear at a private ENT clinic and had had a ventilation tube inserted four months before visiting this clinic. Before the insertion, he had mild conductive hearing loss on the left (Figure 2(a)). He had been given a total of four bottles of Rindelon A® ear drops because of occasional ear discharge through the ventilation tube. An otoscopic examination found that the ventilation tube had been placed in the antero-inferior quadrant of the left tympanic membrane, through which the mucoperiostium in the middle ear looked intact, and that there was no discharge. A pure-tone audiometric examination showed profound hearing loss on the left (Figure 2(b)). Neuro-otological examination found no

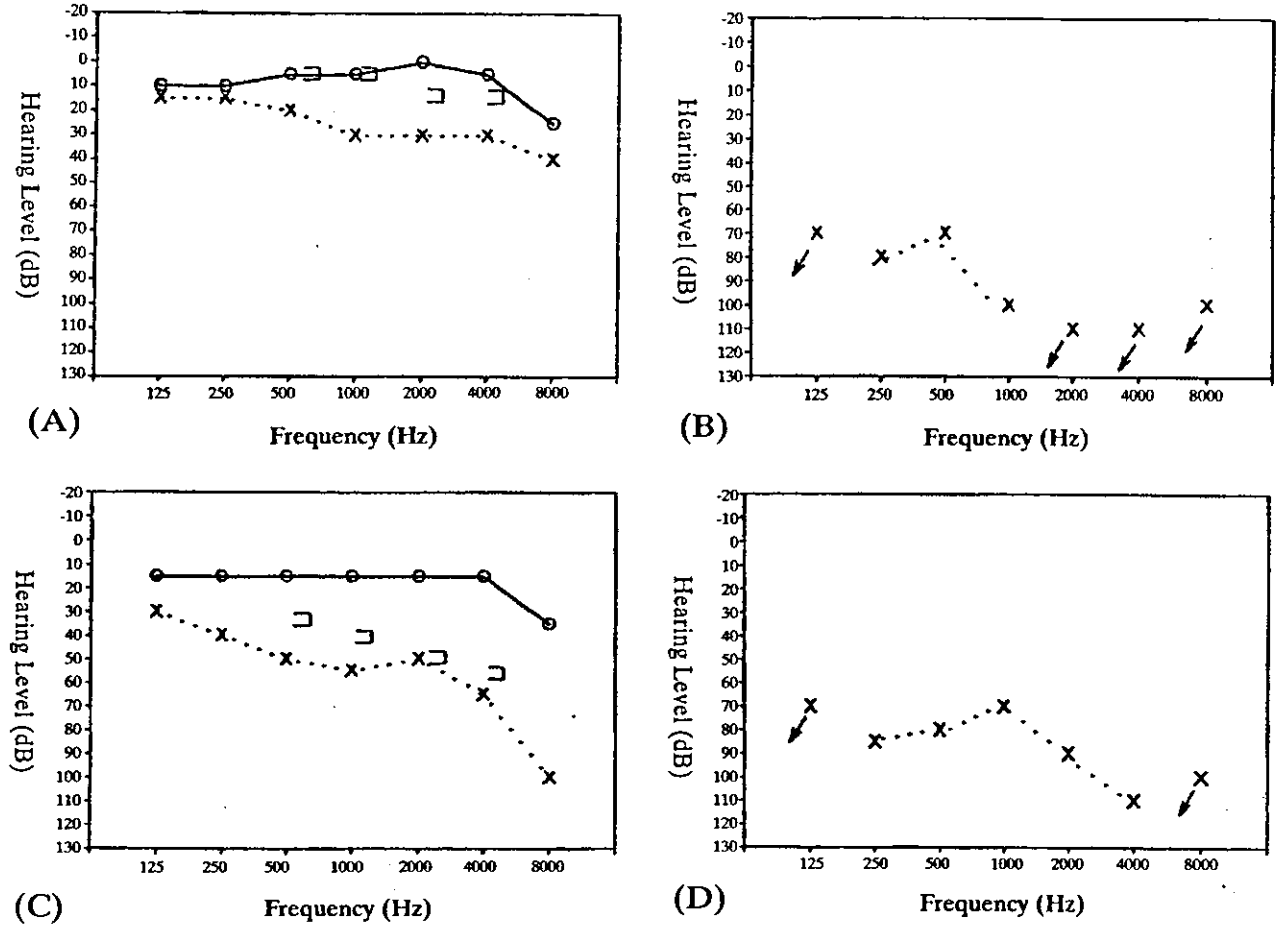

FIG. 2

(a) Mild conductive hearing loss on the left before the use of Rindelon A® ear drops in *Case 2*. (b) Profound mixed hearing loss on the left in *Case 2* after the use of Rindelon A®. (c) Moderate mixed hearing loss on the left in *Case 3* after the use of Rindelon A® ear drops. (d) Deterioration of hearing in *Case 3* seen four months after the use of the ear drops.

abnormalities. An ENG recorded no spontaneous, positional or positioning nystagmus. A caloric testing with 5 ml cold (4°C) saline produced nystagmus with a slow component velocity of approximately 35°/s and 40°/s on stimulation of the right and left ear, respectively. Brain MRI with Gd-DTPA enhancement showed no abnormalities. The use of these eardrops was stopped, but when he revisited 12 months later, he was found to be completely deaf in the involved ear.

Case 3

A 58-year-old female had been given several bottles of Rindelon A® ear drops at a private ENT clinic six months before visiting this clinic for a serous discharge from her left ear. She experienced tinnitus and hearing loss in the left ear one month after using the eardrops. She had been given additional bottles of these eardrops one month before visiting this clinic, and two weeks after starting the use of these eardrops severe unsteadiness occurred. An otoscopic examination found a small perforation in the postero-superior quadrant of the left tympanic membrane, through which the mucoperiostium in the middle ear appeared to be intact. There was no discharge in the middle or external ear. A pure-tone audiometric examination showed moderate mixed hearing loss on the left (Figure 2(c)). Neuro-otological examinations revealed spontaneous horizonto-rotatory nystagmus, strongly beating to the right. Caloric testing with 5 ml cold (4°C) saline produced nystagmus with a slow component velocity of approximately 30°/s on stimulation of the right ear, but no nystagmus was elicited on stimulation of the left ear with 20 ml cold saline. MRI with Gd-DTPA enhancement showed that there were no intracranial lesions such as a CPA tumour. Despite oral administration of a corticosteroid, ATP, and vitamin B12, spontaneous nystagmus continued over the next four months, and her left-side hearing deteriorated (Figure 2(d)).

Examination for the presence of A1555G point mutation in mtDNA

None of the three patients had close relatives with deafness, but their histories suggested that they might have been hyper-susceptible to aminoglycosides. The authors therefore examined whether any of the patients had an A1555G point mutation in their mtDNAs. The method used has been reported elsewhere.[11] In brief, total DNA was isolated from the patients' peripheral leukocytes. To determine whether the A1555G mutation was present, the mtDNA fragment surrounding the 12S rRNA mutation site was amplified by a polymerase chain reaction (PCR) that used the sense primer 5'-AAACTCAAAGGACCTGGCGG (nt 1160–1179) and antisense primer 5'-CGTCCAAGTCGACTTTCCAG (nt 1598–1579). The fragments obtained were subcloned

into a plasmid vector by use of a TA cloning kit (Invitrogen, San Diego, Calif., USA) then directly sequenced in an ABI DNA sequencer. In the dot-blot hybridization, 2 μl of each amplified DNA was spotted onto nylon filters. A probe of 19-mer oligonucleotides five'-TACGACTTGCCTCCTCTAT (nt 1564–1545) was synthesized and labelled with γ-^{32}P-ATP. The filter was hybridized with the labelled probe in 3 mol tetramethylammonium chloride (TMAC) solution for 3-five h at 55°C. Then the filter was washed twice in rinse buffer at room temperature and twice more in TMAC solution at 58°C. The filter was exposed to Kodak XOMAT film for 1–5 h at –70°C.

Using this method, no abnormal sequences around nt 1555 were found in any of the patients. Moreover, none had the A1555G point mutation.

Discussion

All patients in the present study had a tympanic membrane perforation unaccompanied by inflammatory oedema or discharge in the middle ear. They had received several bottles of Rindelon A® ear drops containing 0.35 per cent neomycin sulphate and 0.1 per cent betamethasone sodium phosphate. Patient 1 noticed hearing loss two months after using Rindelon A® ear drops and her hearing loss progressed nine months after the termination of the eardrop usage. Patient 2 developed profound hearing loss after use of Rindelon A® ear drops over four months and was found to become completely deaf in the involved ear when he revisited 12 months later. Patient 3 noticed hearing loss one month after using Rindelon A® ear drops. She developed moderate mixed hearing loss, which had progressed four months after the termination of the eardrop usage. By means of MRI, the presence of intracranial lesions such as CPA tumour was discounted in all patients. The latency from the onset of therapy and period of progression of hearing loss in these patients are similar to those reported in cases of neomycin ototoxicity.[1,2] The close time relationship between medication and the symptoms and the absence of intracranial lesions strongly suggest that the progressive hearing loss in these patients occurred due to the neomycin included in Rindelon A® ear drops that were applied to the perforated eardrum.

The concentration of neomycin in Rindelon A® eardrops is 0.35 per cent, the same as in Cortisporin® and Pediotic® otic suspensions commonly used in the USA. Despite its low concentration of neomycin, Rindelon A® ear drops induced severe inner ear damage in these patients. Following cessation of the use of this product, all these patients showed gradual deterioration of hearing. Patients 1 and 2 finally became completely deaf in the involved ear. In the involved ear of *Case 3*, vestibular function was virtually abolished. These cases of severe inner ear damage caused by eardrops containing a low concentration of neomycin raised the question whether the patients had hyper-susceptibility to aminoglycosides.

A homoplasmic A1555G point mutation in mtDNA is reported to be associated with maternally inherited aminoglycoside-induced deafness.[9–12] It has been shown using a rho^0 cell system that cells carrying this mutation had very high susceptibility to streptomycin.[13] Even very small amounts of aminoglycoside are reported to cause severe inner ear damage in persons with this mutation.[10–12] Patients with aminoglycoside-induced deafness and those with deafness of middle-age onset unrelated to aminoglycosides usually coexist in families harbouring the A1555G mutation,[9–11] but sporadic cases in which there was no family history of deafness have been reported.[12] Although none of the patients in this study had other family members with deafness, the presence of these sporadic cases suggested that there might have been an A1555G point mutation. MtDNA analysis, however, showed that none of them had the A1555G point mutation. This shows that, even without the hyper-susceptibility to aminoglycosides caused by the A1555G point mutation, patients with a tympanic membrane perforation may develop severe inner ear damage after using eardrops containing neomycin.

- **Previous studies have shown that aminoglycoside hypersensitivity is more severe in patients with a A1555G mutation in mitochondrial DNA**
- **In this paper three patients with tympanic membrane perforation developed ototoxicity following the use of neomycin based ear drops**
- **None of these patients had abnormalities of mitochondrial DNA**
- **These cases served to confirm the need for caution in the application of topical medication in all patients with safe chronic otitis media**

No inflammatory oedema or pus was found in the middle-ear spaces of any of the patients. Eardrops are given usually when abundant pus and oedema are present in the middle ear of patients with a tympanic membrane perforation. A substance diluted by secretion therefore reaches the round window niche, which in such conditions is usually protected by thickening of the submucosal connective tissues. If there is no middle-ear inflammation, as in these patients, topically applied water-soluble substances can readily reach the round window membrane and gain access to inner ear fluids through that membrane. As previously reported,[6] easy access of neomycin solution to the round window membrane in the absence of inflammatory oedema and secretion may be a significant factor that contributes to the serious side-effects.

Acknowledgments

We thank Prof. Kimitaka Kaga, Department of Otolaryngology Head and Neck Surgery, University of Tokyo, for invaluable comments. The work was supported in part by Grants-in Aid for Scientific Research (No. 11557125) from the Ministry of Education, Culture, Sports, Science and Technology of Japan.

References

1 Kavanagh KT, McCabe BF. Ototoxicity of oral neomycin and vancomycin. *Laryngoscope* 1983;93:649–53
2 Ward KM, Rounthwaite FJ. Neomycin ototoxicity. *Ann Otol Rhinol Laryngol* 1978;87:211–5
3 Harada T, Iwamori M, Nagai Y, Nomura Y. Ototoxicity of neomycin and its penetration through the round window membrane into the perilymph. *Ann Otol Rhinol Laryngol* 1986;95:404–8
4 Brummet RE, Harris RF, Lindgren JA. Detection of ototoxicity from drugs applied topically to the middle ear space. *Laryngoscope* 1976;86:1177–87
5 Kohonen A, Tarkkanen J. Cochlear damage from ototoxic antibiotics by intratympanic application. *Acta Otolaryngol (Stockh)* 1969;68:90–7
6 Lind O, Kristiansen B. Deafness after treatment with ear drops containing neomycin, gramicidin and dexamethasone. A case report. *ORL* 1986;48:52–4
7 Kellerhals B. Hörschäden durch ototoxische Ohrtropfen. *HNO* 1978;26:49–52

8 Merifield DO, Parker NJ, Nicholson NC. Therapeutic management of chronic suppurative otitis media with otic drops. *Otolaryngol Head Neck Surg* 1993;**109**:77–82
9 Prezant TR, Agapian JV, Bohlman MC, Bu X, Oztas S, Qiu WQ, *et al.* Mitochondrial ribosomal RNA mutation associated with both antibiotic-induced and non-syndromic deafness. *Nature Genet* 1993;**4**:289–94
10 Usami S, Abe K, Kasai M, Shinkawa H, Moeller B, Kenyon JB, *et al.* Genetic and clinical features of sensorineural hearing loss associated with the 1555 mitochondrial mutation. *Laryngoscope* 1997;**107**:483–90
11 Yamasoba T, Goto Y, Oka Y, Nishino I, Tsukuda K, Nonaka I. Atypical muscle pathology and a survey of *cis*-mutations in patients harboring a 1555 A-to-G point mutation in the mitochondrial ribosomal RNA gene. *Neuromuscul Disord* 2002;**12**:506–12
12 Fischel-Ghodsian N, Prezant TR, Bu X, Oztas S. Mitochondrial ribosomal RNA gene mutation in a patient with sporadic aminoglycoside ototoxicity. *Am J Otolaryngol* 1993;**14**:399–403
13 Inoue K, Takai D, Soejima A, Isobe K, Yamasoba T, Oka Y, *et al.* Mutant mtDNA at 1555 A to G in 12S rRNA gene and hypersusceptibility of mitochondrial translation to streptomycin can be co-transferred to ρ0 HeLa cells. *Biochem Biophys Res Commun* 1996;**223**:496–501

Address for correspondence :
Dr. Tatsuya Yamasoba,
Department of Otolaryngology Head and Neck Surgery,
University of Tokyo, .
Hongo 7-3-1,
Bunkyo-ku,
Tokyo 113,
Japan.

Fax: 81-3-3814-9486
E-mail: tyamasoba-tky@umin.ac.jp

Dr T. Yamasoba takes responsibility for the integrity of the content of the paper.
Competing interests: None declared

The Laryngoscope
Lippincott Williams & Wilkins, Inc.

New Method of Using Reconstructed Images for Assessment of Patency of Intracochlear Spaces for Cochlear Implant Candidates

Shotaro Karino, MD; Naoto Hayashi, MD; Shigeki Aoki, MD; Kuni Ohtomo, MD; Tatsuya Yamasoba, MD

Objective/Hypothesis: **A new method of reconstruction using multidetector-row helical computed tomography (MDCT) was applied for assessment of cochlear patency in cochlear implantation candidates.** ***Study Design:*** **Descriptive study comparing radiologic and surgical findings in eight radiologically normal cochleas and four abnormal cases.** ***Methods:*** **In unusual cases including cochlear ossification and misinsertion of electrodes, intracochlear space was evaluated on two types of reconstructed images: the "basal turn plane" that was vertical to the modiolus and contained whole basal turn was effective in the assessment of the lining of the inner bony wall of the otic capsule; "cochlear cross plane" images allowed evaluation of the patency of the intracochlear space and the location of inserted electrodes at the sections vertical to the direction of insertion of the electrodes.** ***Results:*** **Preoperative evaluation was useful for predicting possible problems in electrode insertion and therefore helped in decision-making in regards to surgical strategies, especially in candidates with a high probability of cochlear ossification such as those with meningitis and otosclerosis. Furthermore, the new reconstruction method also provided useful information on the position of the cochlear implant electrodes after surgery.** ***Conclusions:*** **These unusual cases demonstrated that preoperative MDCT evaluation by our reconstruction method was useful for predicting possible problems in electrode insertion and decision-making in regards to surgical strategies, especially in cochlear implantation candidates with a high probability of cochlear stenosis.** ***Key Words:*** **Multidetector-row helical computed tomography, cochlear implantation, cochlear ossification, otosclerosis, meningitis.**

***Laryngoscope*, 114:1253–1258, 2004**

INTRODUCTION

Partial or total obliteration of the cochlear scalae is frequently encountered in patients with deafness caused by otosclerosis, meningitis, and labyrinthitis.[1] Otosclerosis and meningitis can induce intracochlear changes that range from fibrosis to almost complete obliteration of the cochlea. In suppurative labyrinthitis, fibroblastic proliferation occurs within the perilymphatic spaces in the early period after bacterial penetration and is subsequently followed by ossification. In general, such ossification progresses from the base to the apex, resulting in complete labyrinthitis ossificans.[2]

Severe intracochlear obstructive changes have been found in a limited number of postlingually deaf adults but very commonly in children deafened by meningitis.[3] The House Ear Institute has reported that 64.0% of the 128 children who underwent cochlear implantation have become deaf because of meningitis.[4] In these cases, 21.3% of the cochleae showed radiologic evidence of ossified cochleas, but ossification of scala tympani was confirmed in as many as 33.9% during surgery.

Cochlear ossification evident on radiologic examination had previously been considered as a contraindication to cochlear implantation. The reasons for the contraindications included difficulty in insertion of the electrodes, increased resistance to spread of electrical stimuli, and possible damage to neural elements.[1,5] Since the description of alternative techniques such as the short insertion tunnel technique[6] and total drill-out technique,[1,7] several reports have demonstrated the safety and efficacy of cochlear implantation for patients with ossified cochleae.[5,8,9] The purpose of this report is to describe a new method using multidetector-row helical computed tomography (MDCT) to assess cochlear patency in cochlear implantation candidates, especially those with a high probability of cochlear ossification.

MATERIALS AND METHODS

MDCT was performed before and after cochlear implantation, and reconstructed images were compared with the surgical findings. First, we applied our new method to eight patients who underwent cochlear implantation at our hospital. In both axial and coronal slices of high-resolution computed tomography

From the Department of Otolaryngology (S.K., T.Y.), Head and Neck Surgery, and the Department of Radiology (N.H., S.A., K.O.), Faculty of Medicine, University of Tokyo, Tokyo, Japan.

Editor's Note: This Manuscript was accepted for publication January 21, 2004.

Send Correspondence to Dr. Tatsuya Yamasoba, Department of Otolaryngology Head and Neck Surgery, Faculty of Medicine, University of Tokyo, 7–3-1 Hongo, Bunkyo-ku, Tokyo 113–8655, Japan. E-mail; tyamasoba-tky@umin.ac.jp

(HRCT) and T2-weighted magnetic resonance images (MRI) taken before surgery, all showed no abnormal findings in the cochlea. The scala tympani was found during surgery to be widely open, and cochlear implant (CI) electrodes were inserted smoothly through a standard posterior tympanotomy approach in every case. Here, we describe the procedure used for the multiplanar reconstruction in a typical case. Figure 1 shows the preoperative images of a 9-year-old girl who had become deaf after mumps labyrinthitis 6 months earlier, and Figure 2 shows her images taken before and after insertion of the electrodes.

Axial projections of the temporal bone in both ears were taken in helical scan modes (0.5 mm slice width, 120 kV, 300 mA, pitch 3:1) with a multislice CT that has four detector rows (Toshiba Aquillon 16, New York, NY). The reconstruction spacing was 0.1 mm. The raw data were transferred to a workstation (Advantage Workstation version 4.0; GE Medical Systems, Milwaukee, WI), where three-dimensional (3D) reconstruction was performed. As shown in Figure 1, on the axial slice, in which the center of the modiolus was seen, we set a "basal turn plane" that was vertical to the modiolus and contained whole basal turn (Fig. 1A). Then, guidelines were set to pass through the modiolus on this basal turn plane (Fig. 1B). "Cochlear cross planes" (Fig. 2, A and B) were obtained so that they included both the modiolus and one of the guidelines. By rotating the guidelines around the axis, we could observe cochlear cross plane images consecutively. These reconstructed cochlear cross plane images contained the center of the fundus of the internal auditory meatus (IAM). Eighteen of these images taken every 10 degrees were printed on film. The presence of stenosis of intracochlear spaces caused by ossification or bony growth was evaluated on the basal turn plane images and consecutive cochlear cross plane images. As shown in Figure 1B, the lining of the inner bony wall of the otic capsule appeared smooth preoperatively in these patients on the basal turn plane images. Consecutive cochlear cross plane images showed lack of stenosis of the intracochlear spaces (Fig. 2, A and B). Figure 2, C and D, shows cochlear cross plane images taken after the insertion of 22 intracochlear electrodes and 2 mechanical support bands of the CI (Nucleus 24, Cochlear Ltd., Lane Cove, Australia). The image shown in Figure 2C depicts almost the same slice as the image shown in Figure 2A, and the image shown in Figure 2D corresponds with that shown in Figure 2B. These images clearly show the placement of the electrodes in the basal turn. These reconstructive procedures were performed cooperatively by radiologists and otologists, and a series of images for a subject was obtained in approximately 20 minutes.

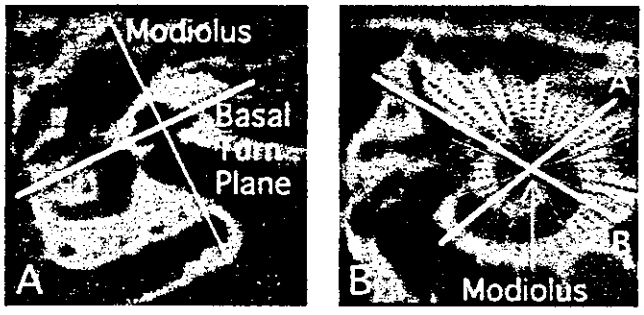

Fig. 1. (A) Preoperative axial slice of a 9-year-old girl in which the center of the modiolus is seen. A basal turn plane that was vertical to the modiolus and contains the whole basal turn is set. (B) The reconstructed basal turn plane image. On this image, the lining of the inner bony wall of the otic capsule is smooth. Guidelines are set to pass through the axis on this plane. Guideline "A" and guideline "B" indicate the cochlear cross planes demonstrated in Figure 2.

CASE REPORTS

We describe four representative cases showing abnormal findings with our reconstruction method.

Case 1

In a 62-year-old male with otosclerosis, axial and coronal HRCT demonstrated the presence of demineralization and destruction of the otic capsule on both sides, typical for the advanced and active phase of cochlear otosclerosis (Fig. 3A). However, it was difficult to determine whether there was space for electrode insertion. The basal turn plane images taken before surgery demonstrated irregular lining of the inner bony wall of the otic capsule in the right ear (Fig. 3B). Severe stenosis and lack of spaces in the lower portion of the basal turns were evident on the preoperative cochlear cross plane images (Fig. 4, A and B). These images also suggested the patency of mainly the scala vestibuli, which was located in the upper half of the basal turn. We explored the promontory in the right ear by the canal wall-up approach and found that the scala tympani around the round window niche were virtually occluded with ossified tissues. Using the transcanal drill-out technique,[7] we made a narrow tunnel, approximately 4 mm long, from the area just superioanterior to the round window niche to the ascending bend of the basal turn, where the patent scala vestibuli was exposed and a small amount of perilymph seepage was observed. Although the cavity of the scala vestibuli was narrow, 22 intracochlear electrodes and the 3 mechanical support bands of the CI (Nucleus 24) could be smoothly inserted into the scala vestibuli. The basal turn plane images (Fig. 3C) and cochlear cross plane images (Fig. 4, C and D) taken after surgery confirmed that the electrode array was fully inserted in the scala vestibuli of the basal turn.

Case 2

A 51-year-old male who had become deaf after meningitis underwent cochlear implantation at our hospital. Preoperative axial HRCT demonstrated chronic otitis media in the left ear and suggested a small lesion of ossification and slight stenosis in the basal turn of the right ear (Fig. 5A). The basal turn plane images taken before surgery also suggested this stenotic lesion (Fig. 5B). By axial and coronal HRCT, it was difficult to ascertain whether there was sufficient remaining space for electrode insertion. However, the cochlear cross plane images clearly demonstrated that the ossification in the basal turn was restricted to the portion near the modiolus and that there was remaining space outside the lesion (Fig. 5C). A total of 24 intracochlear electrodes of the CI (Medel C40+, MED-EL, Innsbruck, Australia) could be smoothly inserted into the scala tympani in the right ear through a routine posterior tympanotomy approach without additional technique. The cochlear cross plane images taken after surgery (Fig. 5D) confirmed that the electrode array was inserted in the remaining space, as observed in the preoperative images.

Case 3

A 16-year-old male visited our hospital complaining of complete deafness. When he was 9 years old, he had become deaf because meningitis accompanying bilateral acute otitis media. He underwent cochlear implantation in the right ear at another university hospital 1 year later. The insertion of 22 intracochlear electrodes of the CI (Nucleus 22, Cochlear Ltd., Lane Cove, Australia) was successful, and he regained hearing. However, his hearing acuity began to deteriorate at age 15, and he was deaf again 3 months before his first visit to our hospital. At the first examination, the electrodes were found exposed in the external auditory canal. Preoperative axial HRCT demonstrated that the electrode array was completely drawn out from the cochlea, and soft tissue density mass was present around the round window

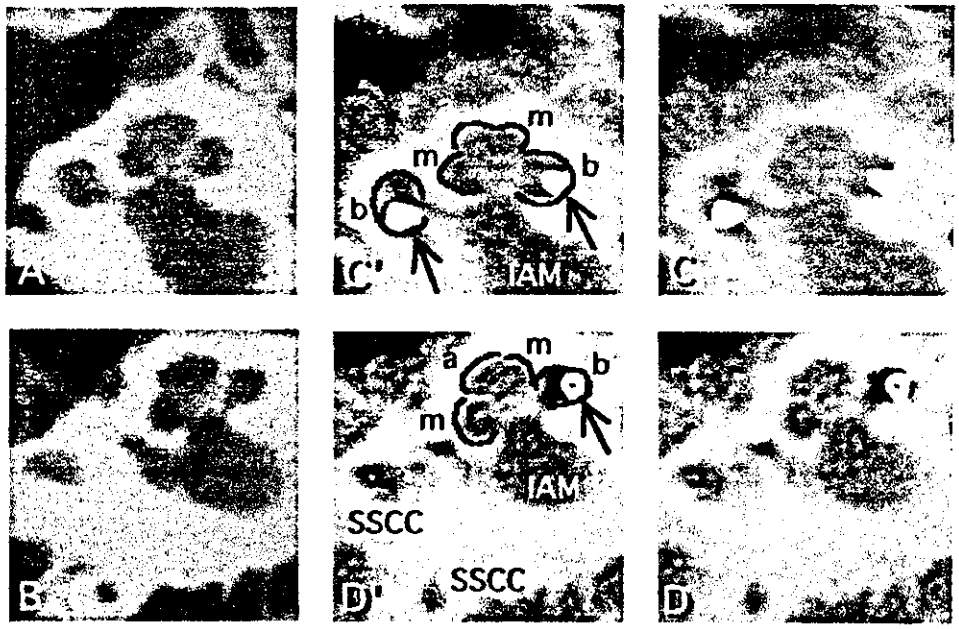

Fig. 2. Cochlear cross plane images of the same patient as demonstrated in Figure 1, taken before and after surgery. (A, B) On the preoperative cochlear cross plane images, note the patency of the intracochlear space of the basal, middle, and apical turns. (C, D) Cochlear cross plane images taken after the insertion of Nucleus 24 and their demonstrative schemes. Image C demonstrates almost the same slice as image A, and image D corresponds with image B. These images clearly show the position of the electrodes (arrows), which were placed in the basal turn (b). The apical turn (a), middle turn (m), internal auditory meatus (IAM), and superior semicircular canal (SSCC) are shown.

(Fig. 6A). To examine whether there was space for electrode reinsertion in the cochlea, we applied our new method of imaging. The basal turn plane images revealed ossification in the basal turn, although the lining of the inner bony wall of the otic capsule appeared smooth, except for the lesion. Severe stenosis and lack of spaces in the basal turns were evident on the cochlear cross plane images (Fig. 6C). Before surgery, we explained to the patient and his family that the reinsertion into the right cochlea might be impossible, and they consented that an option for the opposite side should be prepared for. We explored the tympanum in the right ear through a routine posterior tympanotomy approach and removed the electrode array. After removal of scar tissue in the tympanum, a fenestration into the cochlea was found at the point anterosuperior to the round window niche. Scar tissue was nearly totally removed, but because of the ossification in the intracochlear space, we failed to reinsert a sufficient number of electrodes. Another cochlea implant (Nucleus 24) was fully inserted in the left cochlea.

Case 4

A 58-year-old male was referred to our hospital from another hospital where he underwent cochlear implantation in the left ear. He had become deaf because of meningitis 11 months earlier. According to the surgical record, a fenestration into the intracochlear space was successful, and perilymph seepage was observed. However, the operator found difficulty in inserting electrodes. Only seven intracochlear electrodes of the cochlea implant (Nucleus 24) were inserted. Because satisfactory recognition of speech was not obtained after the implantation, our method of cochlear imaging was requested to investigate the location of the electrodes. A postoperative basal turn plane image revealed that the tip of the array was not in the patent basal turn. The cochlear cross plane images suggested the electrodes were located outside the basal turn (Fig. 7B). 3D images also suggested that the tip had penetrated into the surrounding bony structure (Fig. 7D).

DISCUSSION

Our cases showed that preoperative evaluation of the intracochlear space with MDCT is useful for predicting possible problems in electrode insertion and therefore helps in decision-making in regards to surgical strategies, especially in cochlear implantation candidates with a high probability of cochlear stenosis. The smoothness of the

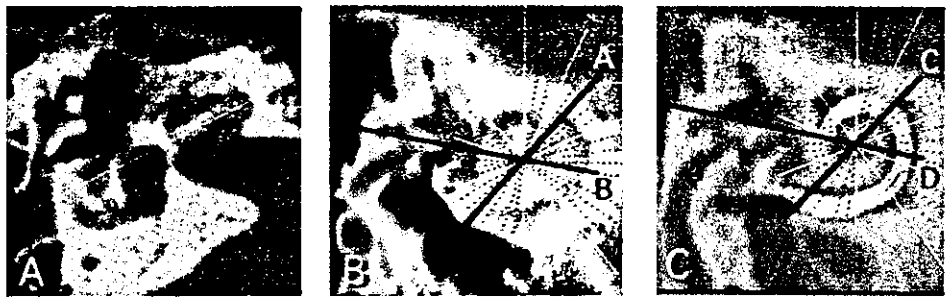

Fig. 3. (A) Conventional axial high-resolution computed tomographic (HRCT) image of a 62-year-old male with otosclerosis (case 1). Note the demineralization and destruction of the otic capsule, typical for the advanced and active phase of cochlear otosclerosis. (B) Preoperative basal turn plane image in case 1. Note the pericochlear lucency and irregular lining of the inner bony wall of the otic capsule. Guideline "A" and guideline "B" indicate the cochlear cross planes demonstrated in Figure 4. (C) Postoperative basal turn plane images taken after the insertion of Nucleus 24 in case 1. This image clearly demonstrates a fully inserted electrodes array in the basal turn. Guideline "C" and guideline "D" indicate the cochlear cross planes demonstrated in Figure 4.

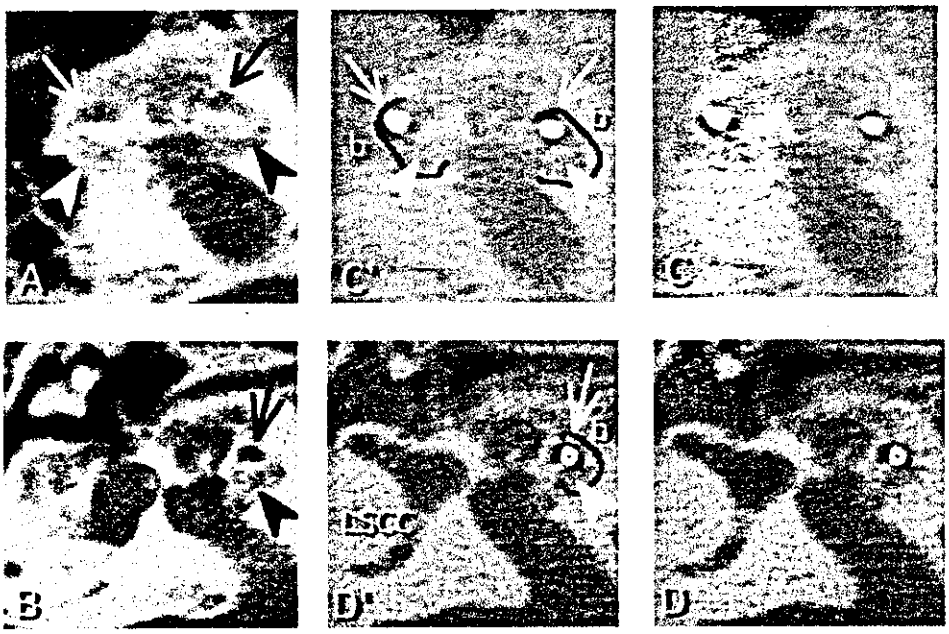

Fig. 4. Cochlear cross plane images taken before and after surgery in case 1. (A, B) Preoperative cochlear cross plane image demonstrates severe stenosis of the lower portion of the basal turns (arrowheads). In contrast, note the patency of the upper portion of the basal turn (arrows). (C, D) Cochlear cross plane images taken after the insertion of Nucleus 24 and their demonstrative schemes (C', D'). Image C demonstrates almost the same slice as image A, and image D corresponds with image B. These images clearly show the position of the electrodes (arrows), which are located in the upper portion of the basal turn (b).

inner wall of the otic capsule in the basal turn could be easily evaluated on the basal turn plane images. The cochlear cross plane images allowed evaluation of the patency of the intracochlear space at the sections vertical to the direction of insertion of the electrodes. In case 1, axial and coronal HRCT demonstrated severe demineralization and destruction of the otic capsule; however, the preoperative cochlear cross plane images demonstrated the area of patent spaces. This finding helped us to determine the most suitable surgical approach for such a difficult case. In case 2, a small lesion of ossification in the basal turn was suggested by axial HRCT, whereas the preoperative cochlear cross plane images showed the remaining space required for insertion of the electrode array. The patency of the intracochlear space in the scala tympani was confirmed during the surgical procedure without additional drilling. Furthermore, the basal turn plane image and the cochlear cross plane image also provided useful information on the position of the CI electrodes after surgery. In case 3, the cochlear cross plane images provided excellent information on patent and ossified areas before reoperation. This information caused us to prepare for cochlea implantation in the opposite unoperated ear before we began the operation to remove the dislocated electrode array. In case 4, the misinsertion of electrodes was clearly recognized on the cochlear cross plane images and also on 3D images in a patient whose hearing acuity did not fully improve.

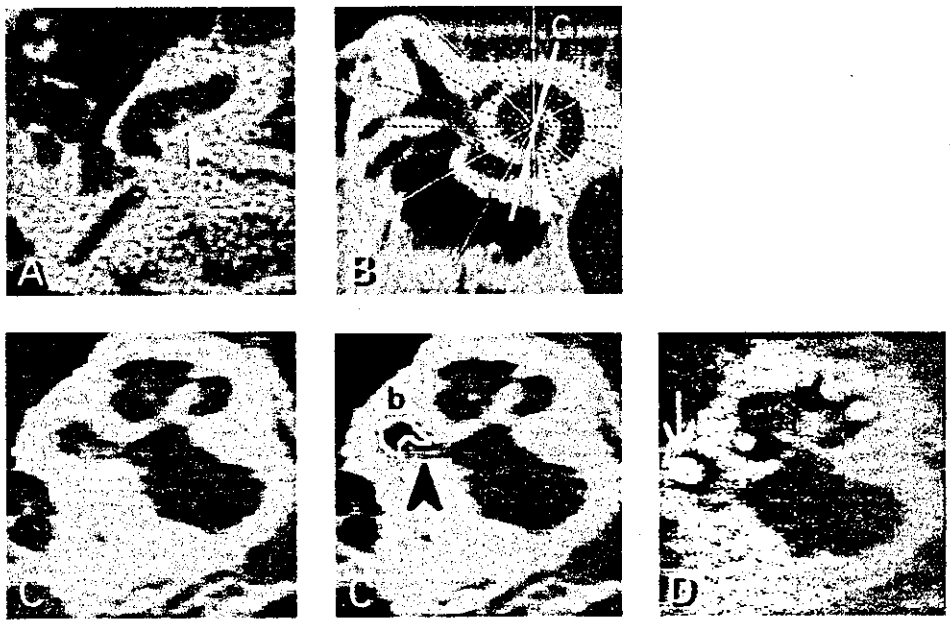

Fig. 5. (A) Axial high-resolution computed tomographic (HRCT) image of a 51-year-old male who had become deaf after meningitis (case 2). Preoperative HRCT suggested a small lesion of ossification (arrowhead) and slight stenosis in the basal turn of the right ear. (B) Preoperative basal turn plane image in case 2. In this image, the lining of the inner bony wall of the otic capsule is smooth except for a small lesion of ossification (arrowhead), which is sectioned on the cochlear cross planes (C) demonstrated in image C. (C) Preoperative cochlear cross plane image and its demonstrative scheme (C'). Ossification (arrowheads) near the modiolus and remaining space outside the lesion in the basal turn (b) are clearly demonstrated. (D) Cochlear cross plane image, which demonstrates almost the same slice as image C, was taken after the insertion of Medel C40+. This image confirms that the electrode array (arrow) was inserted in the remaining space identified in the preoperative image.

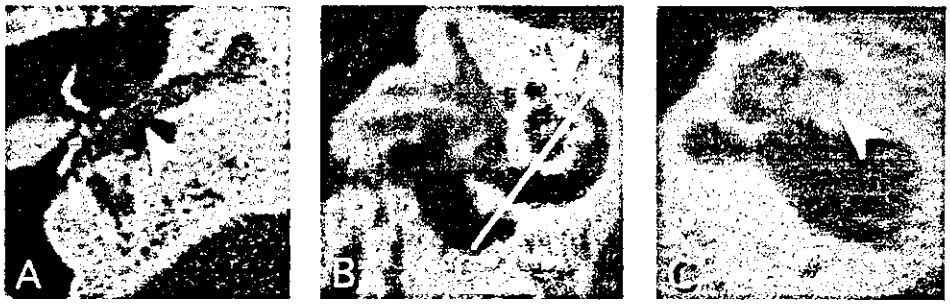

Fig. 6. (A) Axial high-resolution computed tomographic (HRCT) image of a 16-year-old male who had become deaf after meningitis accompanying bilateral acute otitis media (case 3). Preoperative HRCT demonstrated that the electrode array was completely drawn out from the cochlea, and soft tissue density was shown around the round window (arrowhead). (B) Preoperative basal turn plane image in case 3. Ossification in the basal turn (arrowhead) was revealed in this image, although the lining of the inner bony wall of the otic capsule appeared smooth, except for the lesion. Guideline "C" indicates the cochlear cross plane demonstrated in image C. (C) Severe stenosis and lack of spaces in the basal turn (arrowhead) was evident on the cochlear cross plane images.

HRCT of the temporal bone has been considered useful for preoperative evaluation of candidates for cochlear implantation. Abnormal findings such as partial or complete cochlear ossification help to determine the most favorable side for implantation and allow surgeons to anticipate problems that may be encountered during device insertion. However, the two-dimensional (2D) axial images of HRCT cannot completely exclude the possibility of compromised cochlear patency. Small areas of ossification or soft-tissue obliteration in the cochlea, which can be an obstacle to smooth insertion of the electrode, may be missed.[3] Jackler et al.[10] reported a false-negative rate of 46% in their study using 2D axial images. Similarly, Seidman et al.[11] reported that in 32 cases of children with postmeningitis hearing loss, 2D scans with both axial and coronal slices had only a 53% accuracy in detecting intracochlear ossification. The resolution of the inner ear detail obtained by a CT scanner is limited by the width of slices and the partial volume effect. When there is a history of meningitis or otosclerosis in a profoundly deaf person, these disadvantages are not acceptable.

High-resolution T2-weighted MRI of inner ears also provides valuable information of intracochlear space.[12] However, the assessment of detailed configuration of the lining of the inner bony wall of the otic capsule is preferable, especially when the additional drilling technique is expected to be used.

Recent advanced methods for the reconstruction of 3D images allow for significantly better visual recognition of fine structures in the temporal bone. Himi et al.[13] and Reisser et al.[14] have reported that the normal temporal bone structures are clearly recognized on helical CT images. Himi et al.[13] also obtained precise images of CI electrode routes similar to our 3D images in case 4 (Fig. 7D) by varying the angles of view. However, with the aid of an advanced workstation and software equipped with the recent standard device of MDCT, the combination of the basal turn plane images and the cochlear cross plane

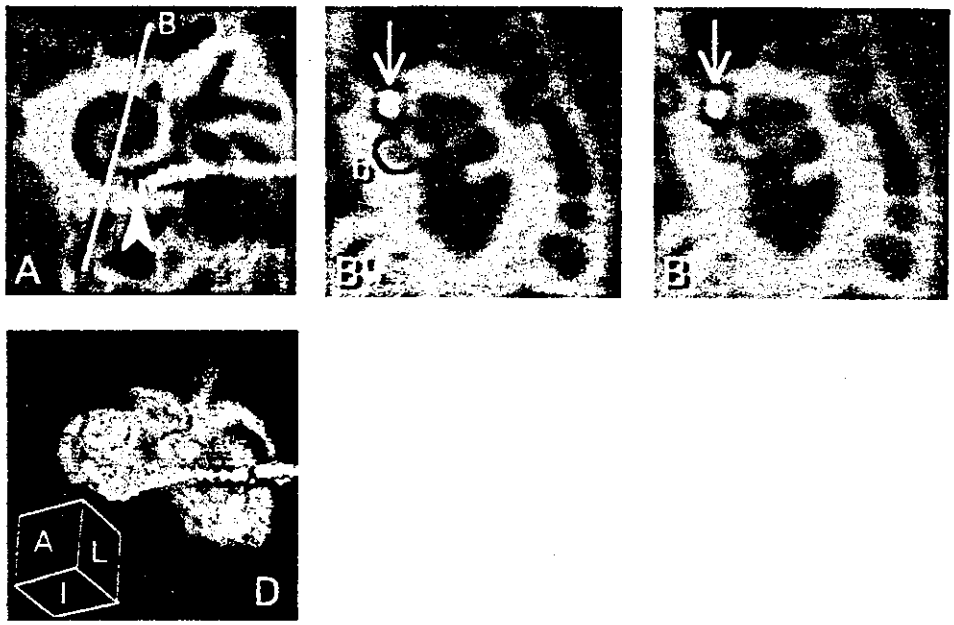

Fig. 7. (A) Postoperative basal turn plane image of a 58-year-old male who regained no satisfactory hearing acuity after cochlear implantation with drilling (case 4). This image shows that the electrode array was penetrating into the bony wall (arrowhead) and that the tip of the array was not in the patent basal turn. Guideline "B" indicates the cochlear cross plane demonstrated in image B. (B) Cochlear cross plane images in case 4 and their demonstrative schemes (B'). These images clearly demonstrated that the electrodes (arrows) were located outside the basal turn (b). (D) Postoperative three-dimensional image of case 4. This image showed that the tip of the electrode array was penetrating into the surrounding bony structure. A, L, and I on the drawn cube indicate the anterior, lateral, and inferior direction, respectively.

images provided additional valuable information to evaluate cochlear patency of the intracochlear spaces. The MDCT protocol used in our study enabled excellent image quality on any reconstructed planes, and our method required neither special technical training nor additional cost for reconstructing the images. MDCT permitted routine use of very thin slices over large regions in short scanning time. The quality of MDCT images appeared to be superior, probably because of less motion artifacts because of the shorter scanning time. However, it was still difficult to discriminate between the scala tympani and the scala vestibuli by preoperative reconstructed images except in special cases, such as case 1.

CONCLUSION

We describe a new reconstruction method using MDCT to assess cochlear patency in cochlear implantation candidates. The excellent results support the routine use of reconstructed MDCT images for evaluation of CI candidates.

BIBLIOGRAPHY

1. Balkany T, Gantz BJ, Steenerson RL, Cohen NL. Systematic approach to electrode insertion in the ossified cochlea. *Otolaryngol Head Neck Surg* 1996;114:4–11.
2. Paparella MM, Sugiura S. The pathology of suppurative labyrinthitis. *Ann Otol Rhinol Laryngol* 1967;76:554–586.
3. Young NM, Hughes CA, Byrd SE, Darling C. Postmeningitic ossification in pediatric cochlear implantation. *Otolaryngol Head Neck Surg* 2000;122:183–188.
4. Luxford WM, House WF. Cochlear implants in children: medical and surgical considerations. *Ear Hear* 1985;6: 20S–23S.
5. Ruckenstein MJ, Rafter KO, Montes M, Bigelow DC. Management of far advanced otosclerosis in the era of cochlear implantation. *Otol Neurotol* 2001;22:471–474.
6. Cohen NL, Waltzman SB. Partial insertion of the nucleus multichannel cochlear implant: technique and results. *Am J Otol* 1993;14:357–361.
7. Balkany T, Bird PA, Hodges AV, et al. Surgical technique for implantation of the totally ossified cochlea. *Laryngoscope* 1998;108:988–992.
8. Steenerson RL, Gary LB. Multichannel cochlear implantation in children with cochlear ossification. *Am J Otol* 1999;20: 442–444.
9. Hodges AV, Balkany TJ, Gomez-Marin O, et al. Speech recognition after implantation of the ossified cochlea. *Am J Otol* 1999;20:453–456.
10. Jackler RK, Luxford WM, Schindler RA, McKerrow WS. Cochlear patency problems in cochlear implantation. *Laryngoscope* 1987;97:801–805.
11. Seidman DA, Chute PM, Parisier S. Temporal bone imaging for cochlear implantation. *Laryngoscope* 1994;104: 562–565.
12. Naganawa T, Koshikawa T, Fukatsu H, et al. Fast recovery 3D fast spin-echo MR imaging of the inner ear at 3 T. *Am J Neuroradiol* 2002;23:299–302.
13. Himi T, Kataura A, Sakata M, et al. Three-dimensional imaging of the temporal bone using a helical CT scan and its application in patients with cochlear implantation. *ORL J Otorhinolaryngol Relat Spec* 1996;58:298–300.
14. Reisser C, Schubert O, Forsting M, Sartor K. Anatomy of the temporal bone: detailed three-dimensional display based on image data from high-resolution helical CT: a preliminary report. *Am J Otol* 1996;17:473–479.

Original Paper

Audiology & Neuro-Otology

Audiol Neurootol 2004;9:282–293
DOI: 10.1159/000080228

Received: September 8, 2003
Accepted after revision: February 20, 2004
Published online: August 13, 2004

Cortical Activation Shortly after Cochlear Implantation

Ken Ito[a] Toshimitsu Momose[b] Shinya Oku[b] Shin-ichi Ishimoto[a]
Tatsuya Yamasoba[a] Masashi Sugasawa[a] Kimitaka Kaga[a]

Departments of [a]Otolaryngology and [b]Radiology, Faculty of Medicine, University of Tokyo, Tokyo, Japan

Key Words
Cochlear implant · Positron emission tomography · Plasticity · Word stimuli · Tone burst stimuli

Abstract
We evaluated the cortical activations in postlingually deaf cochlear implant (CI) users in the early period (0–2 months) of CI usage. The subjects were 8 early CI users and 8 normal subjects. With tone burst stimuli (1 kHz) delivered to the right side, strong and broad activation of the ipsilateral (right) primary auditory cortex with 2 peaks and weaker activation of the contralateral (left) temporal lobe were observed in early CI users, in a clear contrast with the normal subjects in whom activation was observed in a small area of the contralateral (left) primary cortex. With word stimuli, activation of the superior frontomedian cortex presumably including the supplementary motor area and the neighboring cingulate gyri was observed in early CI users, which was absent in normal subjects. The activation in the immediate association cortices near the primary area was lower in early CI users, while the periphery of the association cortex seemed to be more mobilized.

Introduction

The cochlear implant (CI) is an artificial device which restores audition to profoundly deaf patients by directly stimulating the cochlear nerves. In CI users, auditory inputs are resupplied, suddenly at the first switch-on of the cochlear device, to the auditory pathways which are intact but have not been activated for a long period: a candidate condition for evaluating brain plasticity in audition. Positron emission tomography (PET) is a high-resolution imaging method to evaluate quantitatively the local blood flow which represents local synaptic activity. PET is the method of choice for studying CI users, because implanted patients cannot undergo functional MRI studies and because the localization power of electro-/magnetoencephalography remains far inferior to PET [Giraud et al., 2001]. Modified patterns of cortical activation have been reported in CI users with PET studies [Truy et al., 1995; Wong et al., 1999; Giraud et al., 2000; Naito et al., 2000]. The results of these studies, however, were not in perfect agreement, and most of them involved patients already rehabilitated for a relatively long period after implantation. Larger plasticity might be expected in an earlier period, since functional reorganization in the brain was shown in the early stage of idiopathic sudden sensorineural hearing loss, i.e. abrupt deprivation of the neural

KARGER
Fax + 41 61 306 12 34
E-Mail karger@karger.ch
www.karger.com

1420–3030/04/0095–0282$21.00/0

Accessible online at:
www.karger.com/aud

Ken Ito
Department of Otolaryngology, Faculty of Medicine, University of Tokyo
7-3-1 Hongo, Bunkyo-ku
Tokyo 113-8655 (Japan)
Tel. +81 3 5800 8665, Fax +81 3 3814 9486, E-Mail itoken-tky@umin.ac.jp

Table 1. Patient characteristics

Age/gender	Onset age of profound deafness right/left	Cause of deafness	CI usage before PET	Word score %
46/M	43/37	idiopathic (unknown)	1 month	80
58/M	57/57	idiopathic (unknown)	1 week	12
54/M	18/18	streptomycin toxicity	2 weeks	14
43/F	39/39	idiopathic (unknown)	2 weeks	22
45/F	43/25	idiopathic (unknown)	1.5 months	46
44/F	40/40	meningitis	2 weeks	64
53/F	52/52	otospongiosis	1 month	16
54/M	13/at birth	sudden deafness (cochlear aplasia on the left side)	2 months	6

input, an inverse condition to the present study [Po-Hung Li et al., 2003]. A small difference of cortical activations according to the length of use has been shown [Nishimura et al., 2000], but only in the long term (>1 year of use). With early CI users, one report [Giraud et al., 2001] demonstrated smaller cross-modal plasticity in visual cortices in early CI users than in experienced users, and another [Giraud et al., 2001] showed smaller speech-related activation in the auditory cortex compared to rehabilitated users. In adult patients with lesions in the auditory cortices, such as due to infarction and epilepsy, possibly substitutive or compensatory activation of other cortical regions has been observed [Miura et al., 1998; Heiss et al., 1999; Warburton et al., 1999]. Brain plasticity in early CI users, if observed, may also contribute to clarify the mechanisms of such a possible substitution.

In the present study, we evaluated cortical activation in postlingually deaf patients implanted with CI devices by means of PET in an early period (0–2 months) of CI usage, when patterns of brain plasticity might be different from those already found in the later (>6–12 months) period.

Methods

Subjects

Eight normal male subjects (age 24–41 years, average 28.6 years) and 8 postlingually deaf patients implanted with cochlear implant devices (CI users: age 43–58 years, average 49.6 years), 4 males and 4 females, took part in the present study. The normal subjects were all right handed and had normal audition, without any history of psychiatric or neurological disorders. The CI users were also all right handed, were all implanted on the right side with a Nucleus Spectra 22 device but had variable speech intelligibility (single word recognition score: 6–80%, average 32.5%, without lip-reading) using the SPEAK strategy implemented in this device, in which natural spectral characteristics are more preserved, at the time of examination. They were relatively 'naive' users without much experience and rehabilitation with the device (1 week to 2 months after the switch-on of the device, median 24 days). Table 1 shows the patient characteristics. This study was performed in accordance with the guidelines of the Declaration of Helsinki and was approved by the ethical committee of the university hospital.

Tasks and Stimuli

We used 3 conditions: silence, presentation of a train of 1-kHz tone bursts and word presentation. Each condition was repeated twice in a pseudo-random manner in which immediate repetition of the same condition was avoided. During the experiment, the subjects were instructed to close their eyes and silently listen to the sounds when the stimuli were presented, without repeating them in mind. Auditory stimuli were delivered to the right ear of the normal subjects via an ear phone, and to the right cochlea of the CI users via the CI devices. The left ears of the normal subjects were plugged with rubber plugs and covered by headphones, which attenuated the ambient noise by more than 35 dB. The intensity of the sound was adjusted to the so-called comfortable level, the term used in the CI fitting, in which the subject perceives the sound distinctly but does not find it too abrasive (corresponding to 60–70 dB) [Okazawa et al., 1996]. The tone burst stimuli consisted of 1-kHz tone bursts lasting 100 ms, repeated at a rate of 3 Hz. The word stimuli consisted of a series of 3-syllabled Japanese nouns presented at a rate of 1 Hz. The nature of the stimuli had been explained to the subjects, but the stimuli themselves were not presented beforehand, nor was the order of presentation of stimuli. The subjects were asked to report the nature of stimuli after each PET scanning. All the CI users as well as the normal subjects reported the right answers for all stimuli.

PET Acquisition

Regional cerebral blood flow (CBF) was measured using the Headtome-IV system [Iida et al., 1989], following an intravenous bolus injection of $H_2{}^{15}O$ (1480 MBq). Detailed procedures to acquire PET images appear elsewhere [Sakurai et al., 1996]. Briefly, the sound stimuli started 15 s before the scanning began and lasted for

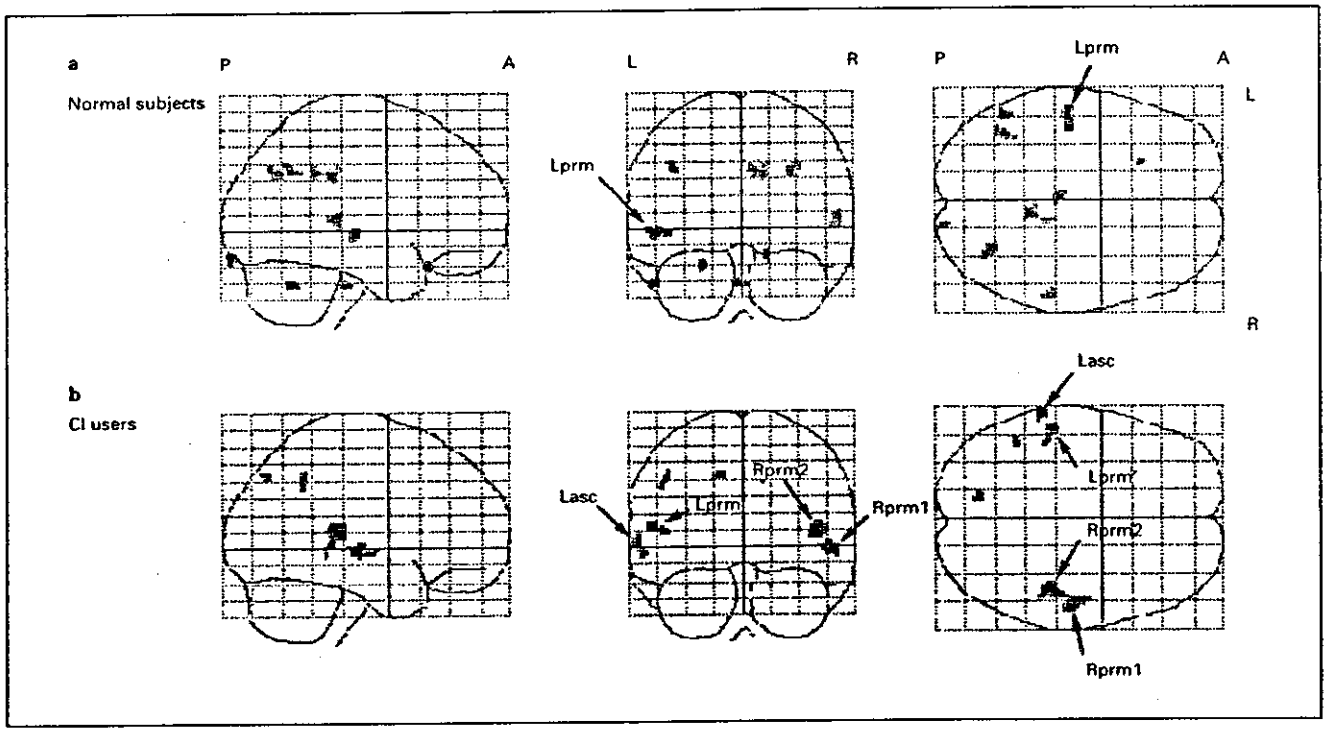

Fig. 1. Projection images of statistical parametric maps, showing activation with tone burst stimuli in normal subjects (**a**) and CI users (**b**). The activated areas were thresholded at uncorrected $p < 0.001$, in order to show clearly the steep activation evoked by this pure-tone-like stimulus. P = Posterior; A = anterior; L = left; R = right. For abbreviations of brain areas, see text.

Table 2. Foci of maximal activation by tone burst stimuli within temporal lobes are shown in the order of Z values calculated by SPM99

	Area	Z value	Coordinates (x, y, z)
Normal subjects	Lprm	4.50	(–50, –20, 2)
CI users	Rprm1	4.42	(54, –20, –2)
		3.30	(50, –21, –4)
	Rprm2	4.36	(44, –32, 10)
	Lprm'	3.84	(–54, –30, 12)
	Lasc	3.84	(–62, –36, 0)

Lprm = Left primary auditory cortex (indicated as Lprm in normals and Lprm' in CI users); Rprm = right primary auditory cortex (Rprm1 and Rprm2: anterolateroinferior and posteromediosuperior portions of the right primary auditory cortex, respectively, in CI users); Lasc = left auditory association cortex. Coordinates (mm) are shown in the standard stereotaxic space of Talairach. Only the areas with peak Z values exceeding 3.3 are shown, i.e. $p < 0.0005$.

60 s, and the scanning lasted for 90 s. Fourteen slices with a pixel size of 2 × 2 mm were obtained. The center-to-center slice distance was 6.5 mm. The CBF was measured based on Kety's single-compartment model. To compute the CBF precisely, arterial radioactivity was monitored with an on-line β+ detector at the rate of 8 ml/min to provide an arterial time-radioactivity curve. The regional CBF values were normalized so that the whole CBF was constant (40 ml/100 g/min).

Data Analyses

Each set of 14 PET images was linearly interpolated into 53 slices (slice distance: 1.6 mm) and then converted to a format compatible with the SPM99 software (Statistical Parametric Mapping, realized by the Wellcome Department of Cognitive Neurology, Hammersmith Hospital, London, UK) [Friston et al., 1991, 1994, 1995; Frackowiak et al., 1997], using the Igor Pro software (Wavemetrics Inc., USA). The standard pre-processings (realignment, normalization to the standard stereotaxic space [Talairach and Tournoux, 1988] and smoothing) and the statistical analyses were performed using SPM99 running on the Matlab 5.2.1 software (Mathworks Inc., USA) for the Windows 98 operating system (Microsoft Corp., USA). The positions of anterior and posterior commissures, necessary for these analyses, were determined by coregistration of PET images with MRI images of each subject, except 1 normal subject in whom

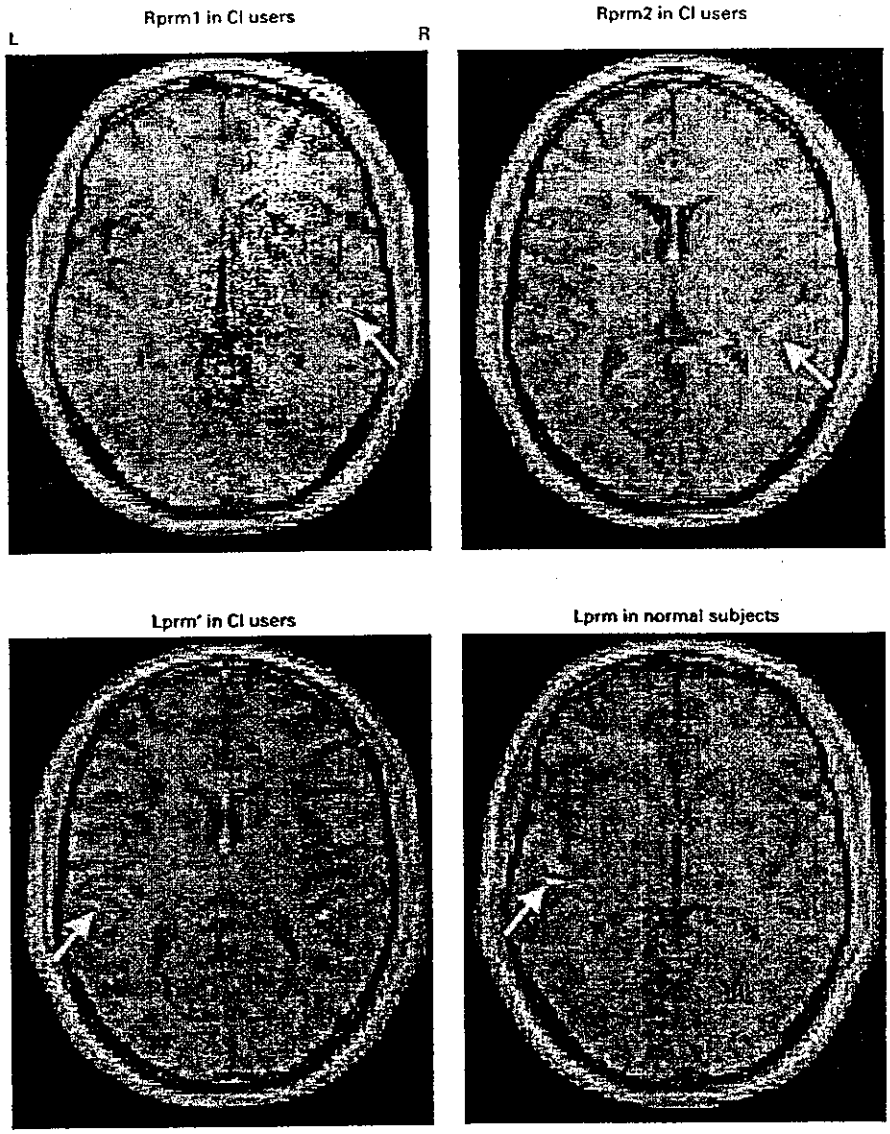

Fig. 2. Activated foci in the primary auditory area with tone burst stimuli. Each focus (Rprm1, Rprm2, and Lprm' in CI users and Lprm in normal subjects) determined by SPM99 are superimposed on the 'canonical' (typical) MRI images registered in SPM99.

MRI was unavailable. In this subject, the anterior-posterior commissure line was determined directly from the PET image. Statistical inference consisted of t tests at each voxel in the brain, which gave p and Z values for each voxel. A smaller p value or larger Z value represents stronger activation.

Activated brain areas were statistically determined by SPM99, which is based on statistical parametric maps using the general linear model. Both in normal subjects and CI users, the two conditions, silence and stimulation, were compared, and the brain areas activated by the stimuli were revealed. SPM is a statistical method developed to avoid the inevitable arbitrariness accompanied by the conventional region of interest method [Friston et al., 1995]. SPM can extract the essential activation related to a certain condition, eliminating the unimportant or noisy activation caused by individual differences etc. We chose this method because of this advantage and because previous CI PET studies also employed this method, and did not discuss the activation case by case, which may permit numerous arbitrary interpretations.

Results

Brain Activation by Tone Burst Stimuli

Tone burst stimuli (table 2) activated a small area in the left primary auditory cortex (Lprm, transverse temporal gyrus) in the temporal lobe of normal subjects (fig. 1a).